Magnetically Enhanced Exciton-Exciton Correlations in Semiconductors

P. Kner, S. Bar-Ad, M. V. Marquezini, and D. S. Chemla
Department of Physics, University of California at Berkeley, Berkeley, California 94720
and Materials Sciences Division, Lawrence Berkeley National Laboratory, Berkeley, California 94720

W. Schäfer
Höchstleistungsrechenzentrum Forschungszentrum Jülich, Jülich, Germany
(Received 4 September 1996)

We present investigations of fs time resolved coherent wave mixing under high magnetic field. Our experiments reveal a new regime at high magnetic field and low excitation density dominated by the Coulomb interaction. This regime is inconsistent with the semiconductor Bloch equations. A model which includes exciton-exciton correlation successfully describes many features of this regime. [S0031-9007(97)02390-9]

PACS numbers: 71.35.Ji, 71.45.Gm, 78.20.Ls, 78.47.+p

Effects associated with quantum confinement have been at the center of interest of solid state physics over the last two decades. In particular, quantum confinement modifies near band-gap optical processes in semiconductors in a nontrivial manner, which has been investigated with great success using time-resolved nonlinear optical spectroscopy [1,2]. Experiments of this type [3,4] have triggered a wealth of theoretical activities [5–8].

In a given semiconductor, almost all the processes influencing the near gap nonlinear response, Pauli blocking (PB), static Coulomb interaction, and Coulomb correlation (CC) (screening, collisional broadening, exciton-exciton interaction) are normally determined by the fixed material parameters. Application of a high magnetic field provides a perfect laboratory for studying the confinement dependence of these fundamental processes which govern the nonlinearities of semiconductors.

When a magnetic field, $\vec{B}$, is applied to a semiconductor, the lowest energy excitons remain Lorentzian, whereas the resonances at the onset of the high energy Landau edges exhibit Fano interference [9,10]. The magnetic field does not change the nature of Lorentzian excitons (LX), but strongly affects their internal structure, contracting the relative motion wave functions, $\phi_\nu(r)$, by a factor $\propto|\vec{B}|^{1/2}$ perpendicular to the field, and by a factor $\propto\ln|\vec{B}|$ parallel to it [11]. This confinement is expected to affect their nonlinear optical response. The effect of a magnetic field on dephasing has been studied in the inhomogeneously broadened $In_xGa_{1-x}As$ ternary alloy [12].

In this Letter, we present the first experimental and theoretical investigations of the effect of increasing two-dimensional confinement on the mechanisms that govern the nonlinear optical response of LXs. We used femtosecond (fs) coherent four-wave mixing (FWM) under high magnetic field for studying the model material, gallium arsenide (GaAs). We observed a smooth transition from a regime consistent with the semiconductor Bloch equation (SBE) formalism [5,6] and the dephasing time approximation (for small B and moderate excitation) to a new regime strongly CC dominated (for large B and very weak excitation) where interaction effects beyond two-particle correlation become important [7,8].

We have performed FWM experiments in the standard self-diffraction configuration with co-circularly polarized (σ^-), $\tau_{\text{laser}} = 100$ fs pulses from a Ti-sapphire laser. The polarization configuration was chosen to minimize the effects of bound biexcitons on the FWM. In this polarization configuration the heavy hole (hh) or light hole (lh) cannot form bound biexcitons, but still interact via the Coulomb force in the continuum of scattering states. Two pulses with wave vectors $\vec{k}_1$ and $\vec{k}_2$ generate the FWM signal emitted in the direction $\vec{k}_s = 2\vec{k}_2 - \vec{k}_1$. The pulses are separated by a time delay Δt ($\Delta t > 0$ when the $\vec{k}_1$ pulse arrives before the $\vec{k}_2$ pulse). The intensities of the two beams were adjusted so that $I_{k_1} \approx I_{k_2}$, to keep the exciton density approximately constant as Δt is varied. The samples are optically thin (0.25 μm) high quality GaAs layers grown by molecular beam epitaxy, sandwiched between two AlGaAs layers, antireflection coated on both sides, and glued on a c axis sapphire substrate. They were placed at $T = 1.6$ K in a split-coil magnet with the field, $0 \leq \vec{B} \leq 12$ T, applied perpendicular to the plane of the sample. We have analyzed the FWM signal in three different ways [10]. We measured the temporally and spectrally integrated FWM signal (TI-FWM) as a function of Δt. At fixed Δt, up-conversion of the FWM signal with a reference pulse in a 1 mm BBO crystal allowed us to trace its absolute-time profile, or time-resolved FWM (TR-FWM). Its spectral content was measured, at fixed Δt, with a spectrometer and an optical multichannel analyzer, giving the power spectrum (FWM-PS).

For a homogeneously broadened atomiclike Lorentzian two-level system, whose only nonlinearity is due to PB, the FWM vanishes for $\Delta t < 0$. For $\Delta t > 0$ both the TI-FWM and TR-FWM decay with a time constant $T_2/2$, where T_2 is the dephasing time [13]. Likewise, the FWM-PS is a Lorentzian peak with a width $2\hbar/T_2$. This contribution is present for all material systems, including semiconductors in which, however, the Coulomb interaction produces specific signatures in the exciton's FWM response. It was found experimentally that the TI-FWM does not vanish for $\Delta t < 0$, but grows with a time constant $T_2/4$, and that the TR-FWM is delayed and nonexponential [3]. This behavior is well explained by the SBE formalism which is based on the Hartree-Fock approximation. It shows that the static Coulomb interaction induces a coupling between polarization and population, contributing to FWM for both $\Delta t < 0$ and $\Delta t > 0$ [5]. In the following, we show that the FWM response is completely changed by the enhancement of the exciton-exciton correlation (XXC) at low density and high B even in the absence of the bound biexciton contribution. In this regime the very slow rise time of the TI-FWM signal for $\Delta t < 0$ is no longer determined by the dephasing time, but by the time scale of scattering events between coherently driven excitons. We show as well that these interaction processes also modify drastically the lh and hh contributions to the FWM-PS.

The samples' low-temperature linear absorption spectrum (not shown) exhibits two distinct exciton peaks [9]. They correspond to the lh and hh bands, whose degeneracy has been lifted due to the mechanical stress induced by the sapphire substrate. As $B = 0 \rightarrow 10$ T we see only small variations in the linewidths $\approx$0.8 meV. The hh-lh splitting shows only minor changes with B.

Figure 1 presents a series of TI-FWM measured for $B = 0 \rightarrow 10$ T for a low total density of excitons $N_x \approx 5 \times 10^{15}$ cm^{-3}. For each B the laser was tuned to keep the exciton density constant. It is worth noting that because of the different shifts of the excitons and the band edge, when the laser is tuned to maintain a constant overlap with the exciton resonances, the overlap with the continuum changes, and so does the number of free carriers generated. When $B = 0 \rightarrow 10$ T the signal peak intensity increases by a factor of $\approx$3. For $B = 0$ T one sees a strong asymmetric peak with a small but non-negligible ($\Delta t < 0$) tail extending to $\Delta t \approx -1$ ps, i.e., $\approx 10 \times \tau_{\mathrm{laser}}$. The TI-FWM profile and strength change almost as soon as B is applied. The most striking changes affect the Δt line shape. Let us call S_{TI}^{+} and S_{TI}^{-} the TI-FWM signal observed for $\Delta t > 0$ and $\Delta t < 0$, respectively. As B increases S_{TI}^{-} increases significantly and becomes visible as far as $\Delta t = -9$ ps for $B = 10$ T. The TI-FWM shows a smooth transition between two regimes: low fields, $B \approx 1 - 2$ T, and high fields, $B \geq 7$ T. In the first case, although one oscillation develops around -0.5 ps, the variation of S_{TI}^{-} is essentially exponential. Whereas S_{TI}^{+} exhibits clear quantum beats [14,15] superimposed on an exponential. A line-shape analysis shows that S_{TI}^{+} is well fitted by a function of the form $e^{-\Delta t/\tau^{+}}(1 + C \sin \omega \Delta t)$. The beat period extracted from the fit corresponds very well to the hh-lh splitting seen in the linear absorption. The decay time constant of S_{TI}^{+} is essentially independent of B for all values of B, $\tau^{+} \approx 1.5$ ps. Conversely, the rise time constant of S_{TI}^{-}, τ^{-}, starts for low B at about $\tau^{+}/2$, but then increases steadily with B. In the high-field regime S_{TI}^{-} develops a strongly nonexponential profile. For long Δt the envelope of S_{TI}^{+} experiences significant changes as well, most likely reflecting those seen in S_{TI}^{-}.

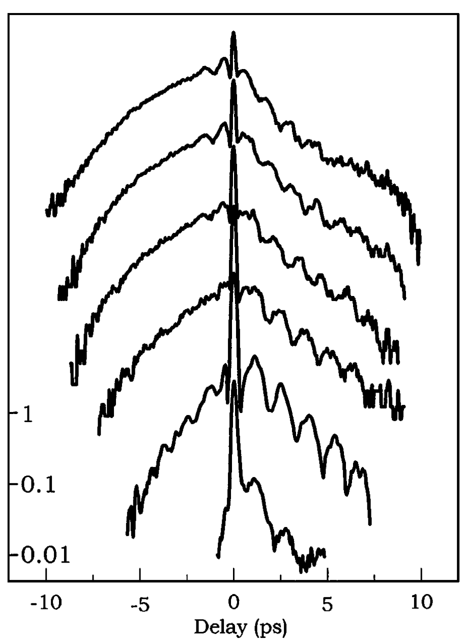

FIG. 1. Time integrated FWM at low excitation density, $N \approx 5 \times 10^{15}$ cm^{-3}, for different magnetic fields. From bottom to top: $B = 0$, 2, 4, 6, 8, and 10 T.

The SBE in the T_2 approximation give a consistent interpretation of the low field regime $B \approx 1 - 2$ T. For a given B, there is an overlap between the laser spectrum and the absorption continuum. Carriers generated in the continuum screen the CC to some extent and induce a collisional dephasing of the excitons that can be characterized by a T_2 [16]. The overall line shape of S_{TI}^{+} and S_{TI}^{-} remains qualitatively the same. As B increases the magnetic confinement affects the exciton internal structure, changing the relative contribution of CC and PB. CC is further enhanced indirectly by the reduction in screening because (i) the carrier motion is more restricted and the exciton "cross section" is reduced and (ii) the laser-continuum overlap decreases so that fewer free carriers are generated. The nonexponential line shape of S_{TI}^{-} is seen in conditions where PB is completely inoperative, $\Delta t \ll -\tau_{\mathrm{laser}}$, and CC is enhanced, $B > 7$ T. As numerical calculations demonstrate, the high-field regime does not lend itself to an interpretation within the SBE formalism, and the TI-FWM decay can no longer be interpreted in terms of a dephasing time.

The extreme sensitivity of the CC-mediated nonlinearity to screening is further demonstrated in Fig. 2. There we present TI-FWM traces obtained at $B = 10$ T for densities $N_x \approx 5 \times 10^{14} \rightarrow 10^{17}$ cm^{-3}. At high and intermediate densities, S_{TI}^{-} and the decay of the S_{TI}^{+} are well-behaved exponentials, as expected in the relaxation time approximation. The corresponding time constants, $\tau^{-} \approx \tau^{+}/2$,

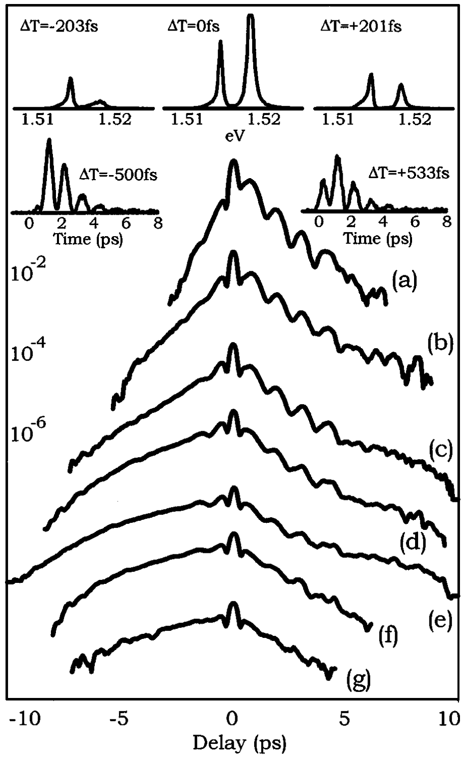

FIG. 2. Time integrated FWM at $B = 10$ T for different excitation densities: (a) $N \approx 10^{17}$ cm^{-3}, (b) $N/2$, (c) $N/3$, (d) $N/6$, (e) $N/20$, (f) $N/63$, and (g) $N/200$. Inset: Time-resolved FWM at $\Delta t = -500$ and $+533$ fs, and FWM power spectra at $\Delta t = -203$, 0, and $+201$ fs; for this data $B = 10$ T, $I_{k_2} \approx 4I_{k_1}$, and $N \approx 10^{16}$ cm^{-3}.

decrease monotonically as the excitation density increases. This behavior is consistent with the SBE regime with collision-induced dephasing [16]. We have verified that at much higher densities, $N_x \approx 10^{18}$ cm^{-3}, where the photocarrier screening dominates, S_{TI}^- disappears altogether. On the contrary, at low density S_{TI}^- is again greater than S_{TI}^+ and clearly nonexponential. The evolution of the curves from high density to low density in Fig. 2 parallels that of the curves from low field to high field in Fig. 1. This similarity confirms our previous conclusions: increasing the magnetic field reduces screening and enhances the CC, resulting in a smooth transition from a regime of screened CC and collision-induced dephasing, consistent with the SBE, to a high-field CC-dominated regime not explained by the SBE theory.

It is surprising to find in the TI-FWM that the quantum beats are very pronounced in S_{TI}^+, whereas S_{TI}^- is pretty much featureless. However, as shown in the inset of Fig. 2, we find that quantum beats are clearly visible in the TR-FWM both for $\Delta t > 0$ and $\Delta t < 0$ as far as $-2.3 \le \Delta t \le +2.7$ ps. Correspondingly, two clear peaks are seen in the FWM-PS at the energies of the hh and lh excitons. The separation between these two peaks agrees very well with the beat period of the TR-FWM. We find that as Δt is varied the hh FWM-PS linewidth, Γ, is on average in reasonable agreement with τ^+, $1/\Gamma \approx 1.5$ ps. We observe, however, significant variations of Γ around that average and more importantly (see inset of Fig. 2) a sensitive dependence of the lh and hh oscillator strength on Δt. It should be emphasized that in the present (σ^-/σ^-) polarization geometry no variation in oscillator strength as a function of Δt occurs in the SBE formalism. The changes in linewidth are also inconsistent with the SBE.

To elucidate the high-field and low density regime we have developed a model that includes XXC. Within the $\chi^{(3)}$ truncation scheme [8,17,18], we express the general kinetic equations [8,17] in the mixed basis of Landau functions and plane waves with $\vec{k} \parallel \vec{B}$, and expand the polarization on the magnetoexciton eigenfunctions. Consistent with the experimental conditions we only consider exciton-exciton scattering states and not bound biexcitons. Also, we include only the contributions of the lowest twofold degenerate lh and hh magnetoexcitons. Furthermore we focus on the coherent limit [17]. With these assumptions the transition amplitudes, P^{eh}, are determined by

$$\left(-i\hbar\frac{\partial}{\partial t} - i\gamma_x - \epsilon_0^{eh}\right)P_0^{eh} = S_{\rm HF} + \sum_{qije'h'} (P_0^{e'h'})^* B_{qij}^{eh'e'h},$$

where $S_{\rm HF}$ describes the usual Hartree-Fock source terms. Except for the last term, this equation represents a multiband nonlinear Schrödinger equation which yields results nearly identical to those of the SBE theory. The term containing the exciton-exciton correlation function, $B_{qij}^{ehe'h'}$, is beyond Hartree-Fock theory [8]. The equation of motion of $B_{qij}^{ehe'h'}$ is driven by products of polarization amplitudes,

$$\left(-i\hbar\frac{\partial}{\partial t} - i\gamma_B - \epsilon_{0i}^{eh}(q) - \epsilon_{0j}^{e'h'}(q)\right)B_{qij}^{ehe'h'} = a_{ij}(q)P_0^{eh}P_0^{e'h'} - b_{ij}(q)P_0^{eh'}P_0^{e'h},$$

where $a_{ij}(q)$ is the second order exciton-exciton interaction matrix element involving the ground state and the i and j exciton states, and $b_{ij}(q)$ is the corresponding exchange contribution. Within the coherent limit these equations are exact and describe rigorously all interaction processes that occur up to the third order in the field, including excitation induced dephasing [19]. An example of the TI-FWM and of several FWM-PS obtained by numerical integration is presented in Fig. 3 which shows that the FWM signal is governed by the XXC. In qualitative agreement with the experiments, the theoretical S_{TI}^- exhibits an extremely slow rise time which is determined by the memory kernel of the correlation function as long as γ_B is not too large. The lowest curve corresponds to the TI-FWM signal calculated without XXC. As compared to the case where XXC is included, the signal is

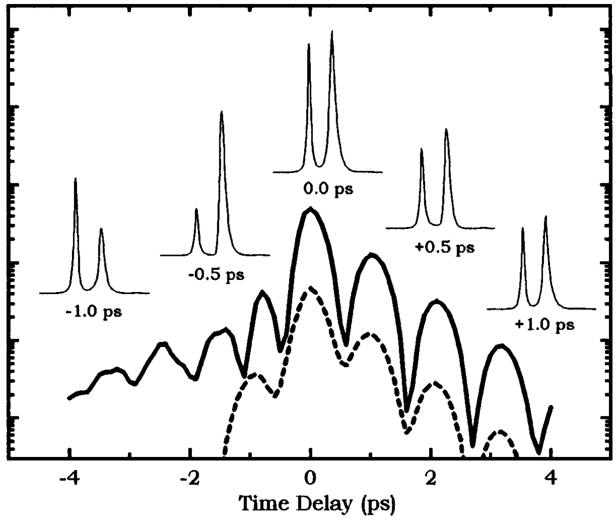

FIG. 3. Theoretical time integrated FWM for $B = 10$ T and low density and FWM power spectra at $\Delta t = -1$, -0.5, 0, $+0.5$, and $+1$ ps. The FWM-PS are not to scale.

about 1 order of magnitude smaller for $0 \leq \Delta t$ and 3 orders of magnitude smaller for large $\Delta t < 0$. This demonstrates the spectacular effects of XXC on the S_{TI}^{-} rise time. If we take screening of the Coulomb interaction within a one-dimensional plasmon-pole approximation into account, the effect of XXC vanishes smoothly with increasing density, as seen experimentally in Fig. 2. Another immediate consequence of XXC is a considerable enhancement of the FWM-PS lh peak due to the different masses occurring in the correlation functions appearing in the $\sum_{qije'h'}$ in the equation of motion of P^{eh}, in contrast to the SBE formalism in which the lh contribution is nearly an order of magnitude smaller than that of the hh. This results in a correlational enhancement of the oscillator strength of the lh and hh which depends sensitively on Δt as observed experimentally. For $\Delta t > 0$ the model shows that the static Coulomb interaction (within the SBE formalism) is responsible for the beats seen in S_{TI}^{+} with little contribution from PB. Beats are also seen in the theoretical S_{TI}^{-}. It is most likely that the attenuation of the beat visibility in the experimental S_{TI}^{-} as well as the nonexponential behavior of the TI-FWM at long Δt have their origin in exciton density correlations which contribute beyond the coherent limit [8,17] and are not included in the model. The model also predicts a strong effect of XXC on the FWM-PS linewidth in agreement with experiments.

In conclusion, we have found that magnetic confinement enhances the effects of Coulomb correlation in coherent wave mixing. We have also found that application of a magnetic field strongly reduces photocarrier screening by restricting their motion and increasing the gap between the excitons and the two-particle continuum. More importantly, we discovered that at very low excitation and high field the nonlinearity is dominated by processes beyond two-particle correlation, and we have presented a theoretical model that explains most of the observed features in terms of exciton-exciton correlation in the scattering state continuum.

We thank Dr. S. Glutsch and Dr. S. Weiss for valuable discussions, and Sandia National Laboratories for the GaAs samples. This work was supported by the Director, Office of Energy Research, Office of Basic Energy Sciences, Division of Material Sciences of the U.S. Department of Energy, under Contract No. DE-AC03-76SF00098.

[1] S. Schmitt-Rink, D. S. Chemla, and D. A. B. Miller, Adv. Phys. **38**, 89 (1989).
[2] *Optics of Semiconductor Nanostructures*, edited by F. Henneberger, S. Schmitt-Rink, and E. O. Göbel (Akademie Verlag, Berlin, 1993).
[3] K. Leo *et al.*, Phys. Rev. Lett. **65**, 1340 (1990); S. Weiss *et al.*, Phys. Rev. Lett. **69**, 2685 (1992).
[4] J.-Y. Bigot, M.-A. Mycek, S. Weiss, R. G. Ulbrich, and D. S. Chemla, Phys. Rev. Lett. **70**, 3307 (1993).
[5] S. Schmitt-Rink and D. S. Chemla, Phys. Rev. Lett. **57**, 2752 (1986); S. Schmitt-Rink, D. S. Chemla, and H. Haug, Phys. Rev. B **37**, 941 (1988); S. Schmitt-Rink *et al.*, Phys. Rev. A **44**, 2124 (1991).
[6] W. Schäfer, in *Optics of Semiconductor Nanostructures*, edited by F. Henneberger, S. Schmitt-Rink, and E. O. Göbel (Akademie Verlag, Berlin, 1993).
[7] V. M. Axt and A. Stahl, Z. Phys. B **93**, 195 (1994); M. Z. Maialle and L. J. Sham, Phys. Rev. Lett. **73**, 3310 (1994); T. Östreich, K. Schönhammer, and L. J. Sham, Phys. Rev. Lett. **74**, 4699 (1995).
[8] W. Schäfer, D. S. Kim, J. Shah, T. C. Damen, J. E. Cunningham, K. Gossen, L. N. Pfeiffer, and K. Köhler, Phys. Rev. B **53**, 16 429 (1996-II).
[9] S. Glutsch, U. Siegner, M.-A. Mycek, and D. S. Chemla, Phys. Rev. B **50**, 17 009 (1994).
[10] U. Siegner, M.-A. Mycek, S. Glutsch, and D. S. Chemla, Phys. Rev. Lett. **74**, 470 (1995).
[11] A. V. Korolev and M. A. Liberman, Phys. Rev. Lett. **72**, 270 (1994).
[12] T. Rappen, G. Mohs, and M. Wegener, Appl. Phys. Lett. **63**, 1222 (1993).
[13] T. Yajima and Yoichi Taira, J. Phys. Soc. Jpn. **47**, 1620 (1979).
[14] K. Leo, T. Damen, J. Shah, E. O. Göbel, and K. Köhler, Appl. Phys. Lett. **57**, 19 (1990).
[15] E. O. Göbel *et al.*, Phys. Rev. Lett. **64**, 1801 (1990).
[16] L. Schultheis, J. Kuhl, A. Honold, and C. W. Tu, Phys. Rev. Lett. **55**, 1635 (1985).
[17] V. M. Axt *et al.*, Phys. Rev. B **53**, 7244 (1996).
[18] M. Lindberg, R. Binder, Y. Z. Hu, and S. W. Koch, Phys. Rev. B **50**, 18 060 (1994).
[19] H. Wang, K. Ferrio, and D. G. Steel, Phys. Rev. Lett. **71**, 1261 (1993).